http://dx.doi.org/10.5012/bkcs.2014.35.7.2193

Nanoparticles Supported-Methylene Blue Labels and Multiwall Carbon Nanotubes-Based Highly Sensitive Electrochemical Immunosensor

A. F. M. Sanaullah,[†] Bongjin Jeong,[†] Rashida Akter,[†] Oc Hee Han,[†,‡] and Md. Aminur Rahman[†,*]

[†]*Graduate School of Analytical Science and Technology (GRAST), Chungnam National University, Daejeon 305-764, Korea*
[*]*E-mail: marahman@cnu.ac.kr*
[‡]*Western Seoul Center, Korea Basic Science Institute, Seoul 120-140, Korea*
Received December 3, 2013, Accepted March 24, 2014

Key Words : Multiwall carbon nanotubes, Electrochemical immunosensor, Gold nanoparticles, Redox label

The detection of proteins at the early stage of diseases plays a very important role in clinical diagnosis, biochemical studies and researches.[1-3] Generally, protein biomarkers have been detected using conventional immunoassays,[4] which are complicated, time-consuming, tedious, expensive, labor-intensive, and not suitable for point-of-care applications. As an alternative to the conventional immunoassay procedures, several immunosensor methods such as surface plasmon resonance (SPR),[5] quartz crystal microbalance (QCM),[6] chemiluminescence,[7] fluorescence,[8] and electrochemistry,[9] have been used extensively for the detection of various disease associated proteins. Among them, the electrochemical immunosensors have been a preferable approach for clinical and environmental immunoassays,[10] due to its high sensitivity and miniaturization. In order to further increase the detection sensitivity, the electrochemical labels need to be used and its amount should be increased. Various nanomaterials such as magnetic nanoparticles,[11] multiwall carbon nanotubes (MWCNTs),[12] silica nanoparticles,[13] carbon spheres,[14] gold nanoparticles (AuNPs),[15] dendrimer,[16] magnetic beads,[17,18] *etc.* have been used as nanocarriers for loading more amount of labels. In most cases, nanomaterial-supported enzymes were used as labels. Although, AuNPs-supported multiple methylene blue molecules (MB) was used as an amplification probe for the impedimetric detection of thrombin (TB) in a $[Fe(CN)_6]^{3-/4-}$ solution,[19] however, the use of nanomaterials-supported and antibody-conjugated MB molecules as an non-enzymatic redox label has not yet been explored in an electrochemical immunosensor.

In the present study, AuNPs-supported anti-hIgG conjugated MB (anti-hIgG/AuNPs/MB) redox label has been prepared for the development of a highly sensitive electrochemical hIgG immunosensor. The AuNPs were used to increase the amount of MB molecules in the bioconjugates. The novelty of this work is to utilize the synergistic effect of nanomaterials-supported MB molecules and the multiwall carbon nanotubes (MWCNTs) as the non-enzymatic electrochemical label and sensor probe, respectively. For the fabrication of the immunosensor probe, hIgG has been immobilized on the chitosan (CS)-coated multiwall carbon nanotubes (MWCNTs) using covalent cross-linking method. The

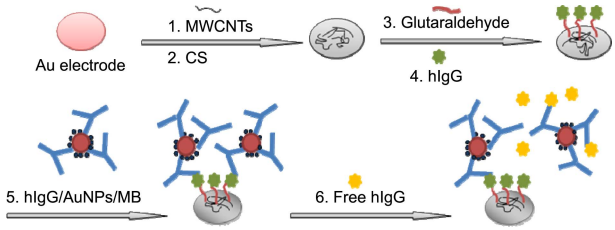

Figure 1. Schematic illustration of the fabrication of hIgG immunosensor.

reasons of using CS and MWCNTs are to prepare a conductive biocompatible probe that has sufficient ability for immobilizing large amounts of biomolecules. Figure 1 shows the schematic illustration of the immunosensor probe. After the immune-interaction of the anti-hIgG/AuNPs/MB redox label with the probe (Au/MWCNTs/CS/hIgG), the MB reduction peak was monitored for the quantitative evaluation of the hIgG concentration in phosphate buffer and human serum sample solutions.

The fabrication of the immunosensor probe was characterized using the scanning electron microscopy (SEM), electrochemical impedance spectroscopy (EIS) and cyclic voltammetry (CV) techniques. Figure 2(A) shows the SEM images obtained for Au/MWCNTs/CS and Au/MWCNTs (inset) surfaces. The SEM image of Au/MWCNTs shows a flat surface where the MWCNTs were agglomerated due to the strong π-π stacking. However, the SEM image of Au/MWCNTs/CS clearly shows a rough surface where the MWCNTs were covered by the CS film without any agglomeration. This indicates that CS prevented the aggregation of MWCNTs through cation-π interaction. The immunosensor surface also characterized by electrochemical impedance spectroscopy (EIS) technique. Figure 2(B) shows the Nyquist plots obtained for the various modified electrodes in 0.1M phosphate buffer solution (PBS) containing 5 mM $Fe(CN)_6^{3-/4-}$. The charge transfer resistances (R_{ct}) were determined from the diameters of the semicircular parts in the high frequency regions of the Nyquist plot. The bare Au electrode exhibited almost a straight line, which is characteristic of a diffusion controlled electron transfer process. The R_{ct} value of Au/CS electrode was about ~3000, which

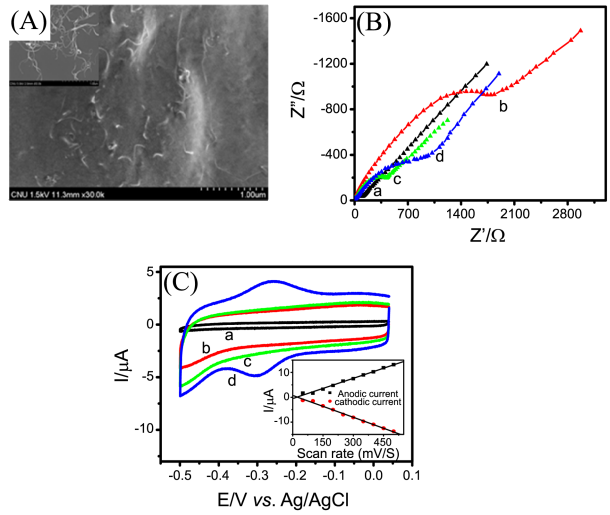

Figure 2. (A) SEM images of Au/MWCNTs/CS and Au/MWCNTs (inset). (B) EIS spectra of (a) bare Au, (b) Au/CS, (c) Au/MWCNTs/CS, and (d) Au/MWCNTs/CS/hIgG electrodes in PBS containing 5 mM $Fe(CN)_6^{3-/4-}$. (C) CVs of (a) bare Au, (b) Au/MWCNTs/CS, (c) Au/MWCNTs/CS/hIgG, and (d) Au/MWCNTs/CS/hIgG/Anti-hIgG/AuNPs/MB electrode in PBS (pH 7.4). Inset shows the scan rate *vs.* current plot.

significantly decreased to 600 in the case of Au/MWCNTs/CS. This indicates that MWCNTs increased the conductivity of the immunosensor surface. However, after the immobilization of hIgG, the R_{ct} value further increased to ~1300. The hydrophobic layer of the protein covers the immunosensor surface and hindered the electron transfer process. The above results clearly indicate that the sensor probe was fabricated successfully. Figure 2(C) shows the CVs recorded for a bare Au (a), Au/MWCNTs/CS (b), Au/MWCNTs/CS/hIgG (c), and an Au/MWCNTs/CS /hIgG modified electrode (immunosensor probe) after binding with anti-hIgG/AuNPs/MB redox label (d) (200 μL) in a PBS solution (pH 7.4). The bare Au, Au/MWCNTs/CS, and Au/MWCNTs/CS/hIgG modified electrodes did not show any redox peaks. The immunosensor probe after binding with the redox label only gave a pair of redox peaks at the formal potential of about −0.28 V, corresponding to the electron transfer (ET) of the MB labels, which were bonded to the immunosensor probe. The redox peak currents were directly proportional to the scan rate between 0.05 and 0.5 V/s. The peak current vs. scan rate plot was linear (inset of the Figure 2(C)), indicating that the redox reaction of MB was involved in a surface-confined process. These results clearly indicate that the ET process of hIgG/AuNPs/MB redox label can be occurred at the immunosensor probe.

The anti-hIgG/AuNPs/MB redox label was characterized using the transmission electron microscopy (TEM) and ultraviolet visible (UV-vis) techniques. Figure 3(A) shows the TEM image of the anti-hIgG/AuNPs/MB redox label, whereas the TEM image of the bare AuNPs is shown in the inset of the Figure 3(A). The sizes of the AuNPs were 4-5 nm, which were separately distributed without any aggregation due to citrate–stabilized negatively charged surface.

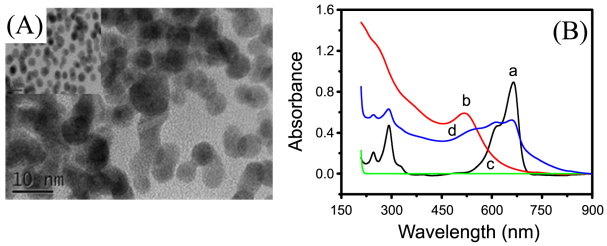

Figure 3. (A) TEM images of hIgG/AuNPs/MB redox label and bare AuNPs (inset). (B) UV-vis absorption spectra of (a) MB, (b) AuNPs, (c) anti-hIgG, and (d) anti-hIgG/AuNPS/MB redox label.

However, after the conjugation with anti-hIgG and MB, the sizes of the AuNPs increased and they were aggregated because of charge neutralization[20] of the positive charges of MB and anti-hIgG and the negative charge of AuNPs. The increased size and aggregation tendency indicates that anti-hIgG and MB conjugated with the AuNPs and formed anti-hIgG/AuNPs/MB redox label. Figure 3(B) shows the UV-vis spectra obtained for (a) AuNPs, (b) MB, (c) anti-hIgG, and (d) anti-hIgG/AuNPs/MB redox label. UV spectrum for the bare AuNPs shows an absorption band at about 525 nm, where as MB shows two absorption bands at 613 and 660 nm. No absorption band was observed for anti-hIgG. In the spectrum of anti-hIgG/AuNPs/MB redox label, both AuNPs and MB bands were observed indicating the successful formation of the anti-hIgG/AuNPs/MB redox label.

The hIgG detection was based on the competitive displacement of the anti-hIgG/AuNPs/MB redox label by the addition of free hIgG. Figure 4(A) shows the SWVs recorded for the immunosensor before (a) and after (b) the displacement reaction. In the presence of the free hIgG, some of the anti-hIgG/AuNPs/MB redox label displaced from the probe surface and interacted with the free hIgG in solution due to the more favorable immunobinding environment. Thus, the amount of MB reduced at the immunosensor surface and the

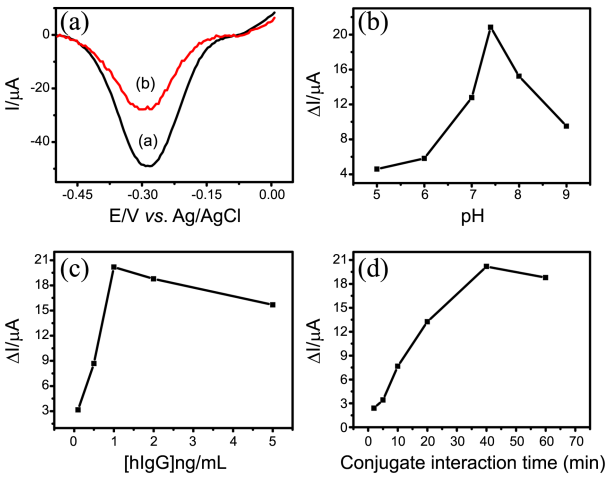

Figure 4. (A) SWV responses (a) before and (b) after addition of free hIgG (10 pg/mL). The effects of pH of the detection medium (B), effect of hIgG concentration during the preparation of the immunosensor (C), and bioconjugate interaction time with immonosensor probe hIgG (D).

current response decreased. The difference in current responses (ΔI) before and after displacement of redox label was taken as the quantitative measure of free hIgG detection. In order to maximize the immunosensor response (ΔI), the experimental conditions such as the pH of the binding medium, the amount of immobilized hIgG on the probe, and the immune-interaction time were optimized. The pH was varied between 5.0 and 9.0 and is shown in Figure 4(B). The ΔI response gradually increased from pH 5.0 to 7.4 and then rapidly decreased over pH 8.0. The decrease of the ΔI responses over pH 8 might be due to the weak immunointeraction at higher pHs. The maximum response was observed at the pH of 7.4 and it was chosen as the optimum pH value for this immunosensor. The effect of hIgG concentration during the preparation of the sensor probe was also optimized. The ΔI responses gradually increased from 0.1 to 1 ng/mL hIgG concentration and over 1 ng/mL hIgG, the ΔI responses decreased slightly (Figure 4(C)). The slight decrease of the ΔI responses may be due to surface saturation occurred at higher concentration of hIgG. Thus, 1 ng/mL hIgG was used to construct the immunosensor. The effect of anti-hIgG antibody and hIgG antigen interaction time, *i.e.*, the interaction time between the bioconjugate and the probe hIgG, was also optimized. The ΔI response gradually increased from 2 to 40 minutes (Figure 4(D)). Over 40 min of interaction time ΔI response did not significantly change. The maximum response was found at 40 min. Thus, 40 min was considered as the optimum interaction time for the bioconjugate and probe binding.

Under the optimized condition, the current responses were measured by varying the free hIgG concentration (Figure 5(A)). The current responses showed a linear inverse relation with the free hIgG concentration. The calibration plot was constructed by plotting the ΔI responses against the logarithmic concentration of free hIgG (Figure 5(B)). The immunosensor exhibited a wide linear range between 10 fg/mL and 20 ng/mL, with a correlation coefficient of 0.98292. The reproducibility expressed in terms of the relative standard deviation (RSD) was about 3.18% (n = 5) at the concentration of 10 pg/mL. The detection limit of the proposed hIgG immunosensor was determined to be 4.0 fg/mL at S/N = 3, which is lower than that of other reported values.[2,3] The addition of other proteins such as PSA, CEA, HRP, and TB did not change the current response significantly, indicating

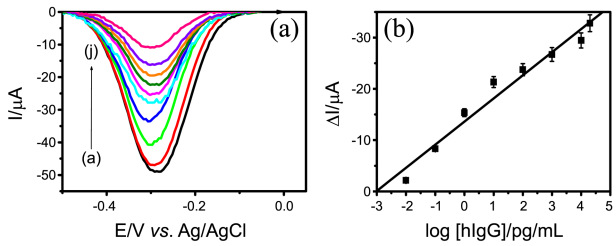

Figure 5. (A) SWV responses before (a) and after (b-j) additions of various concentrations of free hIgG: (b) 0.01, (c) 0.1, (d) 1, (e) 10, (f) 100, (g) 1000, (h) 10000, (i) 20000, and (j) 50000 pg/mL, and (B) the corresponding calibration plot.

that the immunosensor was very specific to hIgG. For evaluating the practical application of the proposed immunosensor, it was applied to hIgG spiked real human serum samples for the detection of hIgG. Excellent recoveries in the range between 97% and 102% were obtained, revealing that the proposed immunosensor can be effectively used in real biological samples.

In conclusion, the proposed anti-hIgG/AuNPs/MB redox label-based electrochemical hIgG immunosensor is highly sensitive, selective, and applicable in real biological samples. It could be a valuable tool for biomarker detection in the field of clinical diagnostics.

Experimental

Reagents and Apparatus. Chitosan (F.W. 340 g), methylene blue (MB), human immunoglobulin G (hIgG) antigen, monoclonal anti-human immunoglobulin G (anti-hIgG) (produced in mouse), prostate specific antigen (PSA), horseradish peroxidase (HRP), carcinoembryonic antigen (CEA), human α-Thrombin (TB), and gold nanoparticles (AuNPs, 4-5 nm in diameter) were purchased from sigma Co. (USA). The multiwall carbon nanotubes (MWCNTs) were obtained from JEIO Co. Korea and purified and shortened according to our previous report.[12] All other chemicals were of extra pure analytical grade and used without further purification. PBS was prepared by mixing Na_2HPO_4 and NaH_2PO_4 with appropriate amount and pH 7.4 was adjusted with a pH meter.

The EIS and SWV experiments were performed using CHI 660 (CH Instruments Inc. USA) and ZAHNER ZENNIUM instrument (Serial no. 40282, Germany) electrochemical work stations, respectively. In SWV, the potential was scanned from +0.3 to −0.5 V with 5 mV pulse height, 50 mV amplitude, and 20 Hz frequency. SWV experiments were performed in an oxygen free PBS buffer solution (pH 7.4) with constant purging of N_2 gas. The SEM and TEM images were obtained using scanning electron microscope (Model JSM-7000F JEOL, Japan) and high resolution transmission electron microscope (Model JEM-2100, JEOL, Japan), respectively. UV-vis experiments were carried out with a UV-vis spectrophotometer (model UV-1800, Shimadzu, Japan).

Preparation of the Au/MWCNTs/CS/hIgG Immuno-Sensor Probe. The immunosensor probe was fabricated by sequentially dropping a 3 μL of purified and shortened MWCNTs and 10 μL of CS (7.5 mg/mL CS in the mixture of 1% HCl and Tris ($NH_2C(CH_2OH)_3$·HCl) buffer, pH 6) solutions on a polished Au electrode. After drying, the Au/MWCNTs/CS modified electrodes were dipped into a glutaraldehyde solution (25%) for 12 h followed by incubated in a PBS solution containing 1 ng/mL hIgG (pH 7.4) for 12 h. By these steps, hIgG were covalently immobilized on the CS film of Au/MWCNTs/CS modified electrode through the glutaraldehyde cross-linking. The modified electrode was carefully rinsed with a PBS solution (pH 7.4) for removing any unbound free hIgG and was blocked with a 0.1% BSA solution for 1 h.

Preparation of the anti-hIgG/AuNPs/MB Redox Label. The anti-hIgG/AuNPs/MB redox label was prepared by incubating the AuNPs in the PBS solutions of MB (0.1 mM) and anti-hIgG (1000 times diluted) for 12 h at 4 °C. The resulting conjugate solution was centrifuged. After discarding the supernatant, the conjugate was carefully washed with PBS (pH 7.4) for three times in order to remove unbound anti-hIgG, MB, and AuNPs. The anti-hIgG and MB were attached on the surface of AuNPs through the charge interaction between the positive charges of MB and anti-hIgG and the negative charge of AuNPs. Finally the anti-hIgG/AuNPs/MB redox label was blocked by using a 0.1% BSA solution for 1 h and was used in the subsequent experiments.

Acknowledgments. This research was supported by the Basic Research Program for Regional University (2012R1A1A4A01007256) and the 2013-University-Institute Cooperation Program funded by the National Research Foundation of the Korean Government (MEST).

References

1. Rosi, N. L.; Mirkin, C. A. *Chem. Rev.* **2005**, *105*, 1547.
2. Mao, X.; Baloda, M.; Gurung, A. S.; Lin, Y.; Liu, G. *Electrochem. Commun.* **2008**, *10*, 1636.
3. Zhang, L.; Liu, Y.; Chen, T. *Int. J. Biol. Macro.* **2008**, *43*, 165.
4. Yates, A. M.; Elvin, S. J.; Williamson, D. E. *J. Immunoassay* **1999**, *20*, 31.
5. Whelan, R. J.; Zare, R. N. *Anal. Chem.* **2003**, *75*, 1542.
6. Kim, N.; Kim, D.; Cho, Y.; Moon, D.; Kim, W. *Biosens. Bioelectron.* **2008**, *24*, 391.
7. Qin, G.; Zhao, S.; Huang, Y.; Jiang, J.; Ye, F. *Anal. Chem.* **2012**, *84*, 2708.
8. Esteve-Turrillas, F. A.; Abad-Fuentes, A. *Biosens. Bioelectron.* **2013**, *41*, 12.
9. Noh, H. B.; Rahman, M. A.; Yang, J. E.; Shim, Y. B. *Biosens. Bioelectron.* **2011**, *26*, 4429.
10. Zhou, C. H.; Long, Y. M.; Qi, B. P.; Pang, D. W.; Zhang, Z. L. *Electrochem. Commun.* **2013**, *31*, 129.
11. Blonder, R.; Katz, E.; Cohen, Y.; Itzhak, N.; Riklin, A.; Willner, I. *Anal. Chem.* **1996**, *68*, 3151.
12. Akter, R.; Rahman, M. A.; Rhee, C. K. *Anal. Chem.* **2012**, *84*, 6407.
13. Lin, M.; Liu, Y.; Liu, C.; Yang, Z.; Huang, Y. *Biosens. Bioelectrons* **2011**, *26*, 3761.
14. Du, D.; Zou, Z.; Shin, Y.; Wang, J.; Wu, H.; Engelhard, M. H.; Liu, J.; Aksay, I. A.; Lin, Y. *Anal. Chem.* **2010**, *82*, 2989.
15. Lai, G. S.; Yan, F.; Ju, H. X. *Anal. Chem.* **2009**, *81*, 9730.
16. Jeong, B.; Akter, R.; Han, O. H.; Rhee, C. K.; Rahman, M. A. *Anal. Chem.* **2013**, *85*, 1784.
17. Akter, R.; Rhee, C. K.; Rahman, M. A. *Biosens. Bioelectron.* **2013**, *50*, 118.
18. Akter, R.; Rhee, C. K.; Rahman, M. A. *Biosens. Bioelectron.* **2014**, *54*, 351.
19. Jeong, B.; Akter, R.; Han, O. H.; Rhee, C. K.; Rahman, M. A. *Bull. Korean Chem. Soc.* **2013**, *34*, 721.
20. Yang, W.; Liu, K.; Song, D.; Du, Q.; Wang, R.; Su, H. *J. Phys. Chem. C* **2013**, *117*, 27088.